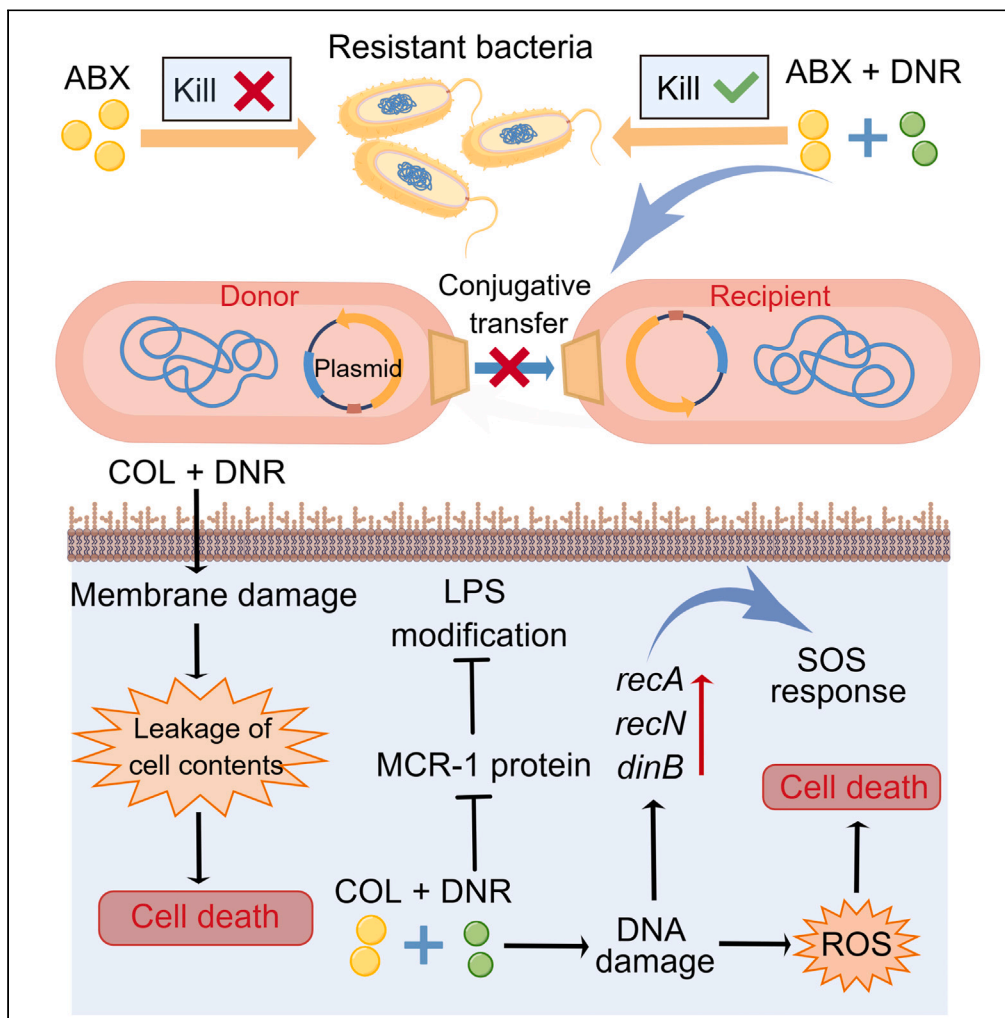


Article

# Daunorubicin resensitizes Gram-negative superbugs to the last-line antibiotics and prevents the transmission of antibiotic resistance



Jinju Cai, Tian Deng, Jingru Shi, Chen Chen, Zhiqiang Wang, Yuan Liu

zqwang@yzu.edu.cn (Z.W.)  
liuyuan2018@yzu.edu.cn (Y.L.)

Highlights

DNR resensitizes drug-resistant bacteria to the last-line antibiotics

DNR thwarts the evolution and transmission of antimicrobial resistance

DNR can directly bind to MCR-1 protein and reduce its expression

DNR plus colistin exacerbates membrane damage and the over-production of ROS



## Article

## Daunorubicin resensitizes Gram-negative superbugs to the last-line antibiotics and prevents the transmission of antibiotic resistance

Jinju Cai,<sup>1,4</sup> Tian Deng,<sup>1,4</sup> Jingru Shi,<sup>1</sup> Chen Chen,<sup>1</sup> Zhiqiang Wang,<sup>1,2,\*</sup> and Yuan Liu<sup>1,2,3,5,\*</sup>

## SUMMARY

Although meropenem, colistin, and tigecycline are recognized as the last-line antibiotics for multidrug-resistant Gram-negative bacteria (MDR-GN), the emergence of mobile resistance genes such as *bla<sub>NDM</sub>*, *mcr*, and *tet(X)* severely compromises their clinical effectiveness. Developing novel antibiotic adjuvants to restore the effectiveness of existing antibiotics provides a feasible approach to address this issue. Herein, we discover that a Food and Drug Administration (FDA)-approved drug daunorubicin (DNR) drastically potentiates the activity of last-resort antibiotics against MDR-GN pathogens and biofilm-producing bacteria. Furthermore, DNR effectively inhibits the evolution and spread of colistin and tigecycline resistance. Mechanistically, DNR and colistin combination exacerbates membrane disruption, induces DNA damage and the massive production of reactive oxygen species (ROS), ultimately leading to bacterial cell death. Importantly, DNR restores the effectiveness of colistin in *Galleria mellonella* and murine models of infection. Collectively, our findings provide a potential drug combination strategy for treating severe infections elicited by Gram-negative superbugs.

## INTRODUCTION

Antibiotic resistance has become the biggest threat to human health in the 21st century.<sup>1,2</sup> Gram-negative bacteria (GNB) show higher intrinsic resistance to many Gram-positive bacteria-active antibiotics because these drugs cannot penetrate the GNB outer membrane.<sup>3,4</sup> Therefore, infectious diseases caused by GNB are more challenging to treat in clinic.<sup>5,6</sup> Carbapenems are one of the main treatments for severe drug-resistant GNB infections. However, New Delhi metallo- $\beta$ -lactamase1 (NDM-1) was discovered in 2009, and it has spread widely in more than 70 countries around the world, seriously weakening the efficacy of carbapenems.<sup>7</sup> To combat the increasingly multidrug-resistant (MDR) GNB, colistin, and tigecycline have been applied in clinical treatment successively as the last line of defense. In clinical practice, the cationic cyclic peptide antibiotic colistin can be used for the treatment of various infectious diseases, including peritonitis, sepsis, and post-burn infections.<sup>8,9</sup> By contrast, complicated skin and skin structure infections (cSSSI) or complex intra-abdominal infections (cIAI) in adults are treated with tigecycline, the first medication in the glycyctetracycline class approved by FDA in 2005.<sup>10</sup> In recent years, plasmid-mediated *mcr-1*<sup>11</sup> and *tet(X3/X4)*<sup>12</sup> were discovered in 2015 and 2019, respectively, which can be transferred to *Escherichia coli*, *Klebsiella pneumoniae*, and other clinical pathogens, resulting in the widespread of colistin/tigecycline resistance. Heretofore, there are no effective drugs available to deal with complex drug-resistant bacterial infections. Therefore, new strategies are urgently needed to counteract the antimicrobial resistance (AMR) threat.

Antibiotic therapy is currently the dominant treatment for bacterial infections.<sup>13</sup> However, the current research and development capabilities of new antibiotics are seriously insufficient, and finding new antibiotics with distinct targets is getting harder, especially for GNB.<sup>14</sup> Besides, high costs and long cycles limit the development of new medicines.<sup>15</sup> Only a small number of novel antibiotics such as daptomycin have been approved by FDA in recent decades.<sup>16</sup> Comparatively, identifying novel antibiotic adjuvants from previously approved compounds (PACs) offers a viable strategy for preserving antibiotic efficacy.<sup>17–19</sup> Moreover, the low cost and good safety, as well as the favorable pharmacokinetic properties of PACs, make them attractive antibiotic adjuvant candidates for translational application. Historically, classical  $\beta$ -lactamase inhibitors such as clavulanate, sulbactam, and tazobactam, effectively prevent the hydrolysis

<sup>1</sup>Jiangsu Co-innovation Center for Prevention and Control of Important Animal Infectious Diseases and Zoonoses, College of Veterinary Medicine, Yangzhou University, Yangzhou 225009, China

<sup>2</sup>Joint International Research Laboratory of Agriculture and Agri-Product Safety, the Ministry of Education of China, Yangzhou University, Yangzhou 225009, China

<sup>3</sup>Institute of Comparative Medicine, Yangzhou University, Yangzhou 225009, China

<sup>4</sup>These authors contributed equally

<sup>5</sup>Lead contact

\*Correspondence: zqwang@yzu.edu.cn (Z.W.), liuyuan2018@yzu.edu.cn (Y.L.)

<https://doi.org/10.1016/j.isci.2023.106809>



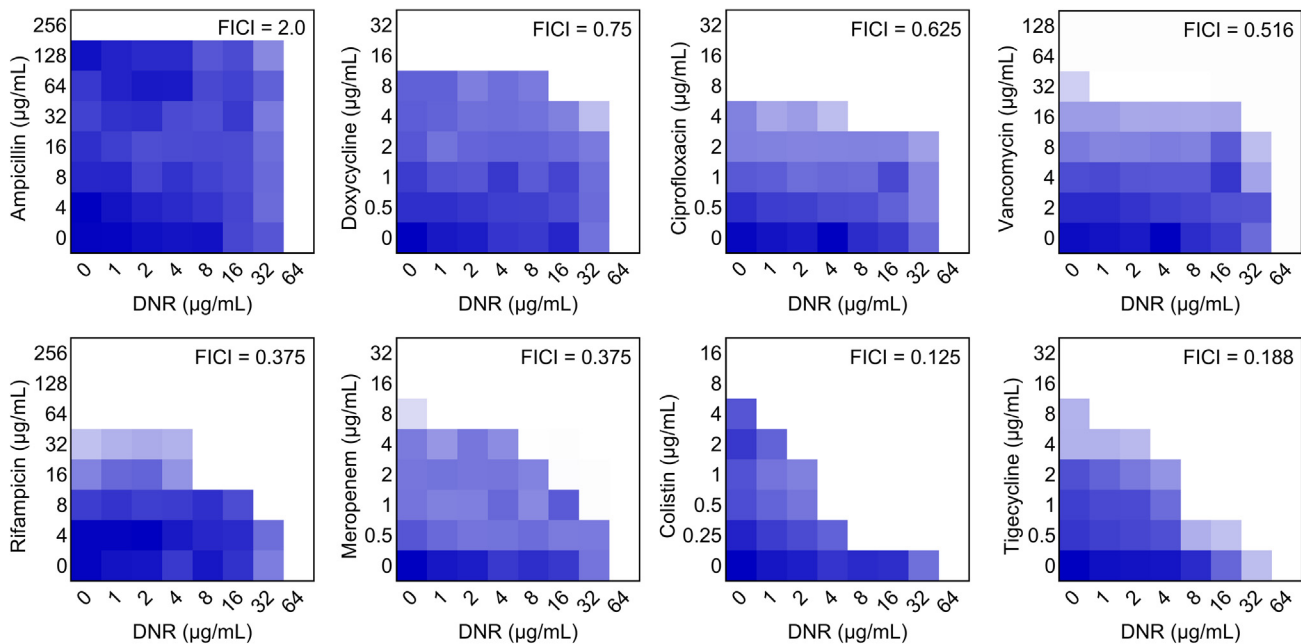


**Figure 1. Checkerboard assay of the synergistic effect of DNR with various antibiotics against multidrug-resistant (MDR) *E. coli* B2 or with tigecycline against *tet(X4)*-carrying *E. coli* B3-1**

Dark blue areas show greater cell density. The data show the average optical density (OD) of two biological replicates (600 nm). An FIC index of less than 0.5 is used to define synergy.

of antibiotics by inhibiting  $\beta$ -lactamase activity,<sup>20</sup> which obtain proven success in the clinic over the past decades. Additionally, some progress has been achieved in the development of new antibiotic adjuvants in recent years. For instance, the natural substance aspergillomarasmine A (AMA), which was once an angiotensin-converting enzyme (ACE) inhibitor, recovers the efficacy of meropenem against NDM-positive Enterobacteriaceae.<sup>21</sup> Owing to the substitution of bismuth on zinc ions in the active center of NDM-1, bismuth nitrate shows excellent synergistic antibacterial action with meropenem.<sup>22</sup> Additionally, by removing bacterial biofilms, triclosan improves the antibacterial action of tobramycin against *Pseudomonas aeruginosa*.<sup>23</sup> Apparently, combining antibiotics with their potentiators screened from PACs offers a new pipeline to defeat the increasing resistance crisis.

Daunorubicin (DNR) is an FDA-approved antitumor drug for treating acute myeloid or lymphocytic leukemia.<sup>24,25</sup> Several previous studies have partially demonstrated the antibacterial effects of DNR against Gram-positive and Gram-negative bacteria,<sup>26,27</sup> while its therapeutic potential as an antibiotic adjuvant remains elusive. Here, we discovered that DNR significantly enhances the effectiveness of the last-resort antibiotics against MDR GNB. Their combination effectively reduces the bacterial loads of drug-resistant bacteria, inhibits the formation of biofilm, and removes mature biofilm bacteria. In addition, DNR remarkably suppresses the evolution and spread of colistin/tigecycline resistance. Mechanistic studies showed that DNR assists colistin to destroy the integrity of the cell membrane of drug-resistant bacteria, subsequently causes DNA damage, induces oxidative damage, and eventually leads to bacterial cell death. Importantly, DNR improves the *in vivo* effectiveness of colistin in animal infection models. The identification of DNR as an antibiotic adjuvant provides a new solution to alleviate the growing crisis of bacterial resistance.

## RESULTS

### DNR displays excellent synergistic activity with meropenem/colistin/tigecycline

Using checkerboard assays, we first investigated the synergistic action of DNR with eight kinds of antibiotics against MDR *E. coli* B2 (*bla<sub>NDM-5</sub>* + *mcr-1*) or tigecycline-resistant *E. coli* B3-1 (*tet(X4)*). The results showed that DNR potentiated the activity of meropenem, rifampicin, colistin and tigecycline (fractional inhibitory concentration index [FICI]: 0.375, 0.375, 0.125, and 0.188, respectively), of which the synergistic activity with colistin was the strongest, followed by tigecycline, whereas had only weak synergistic activity or no activity with the other four antibiotics (FICI > 0.5) (Figure 1). To reveal whether the synergistic activity of

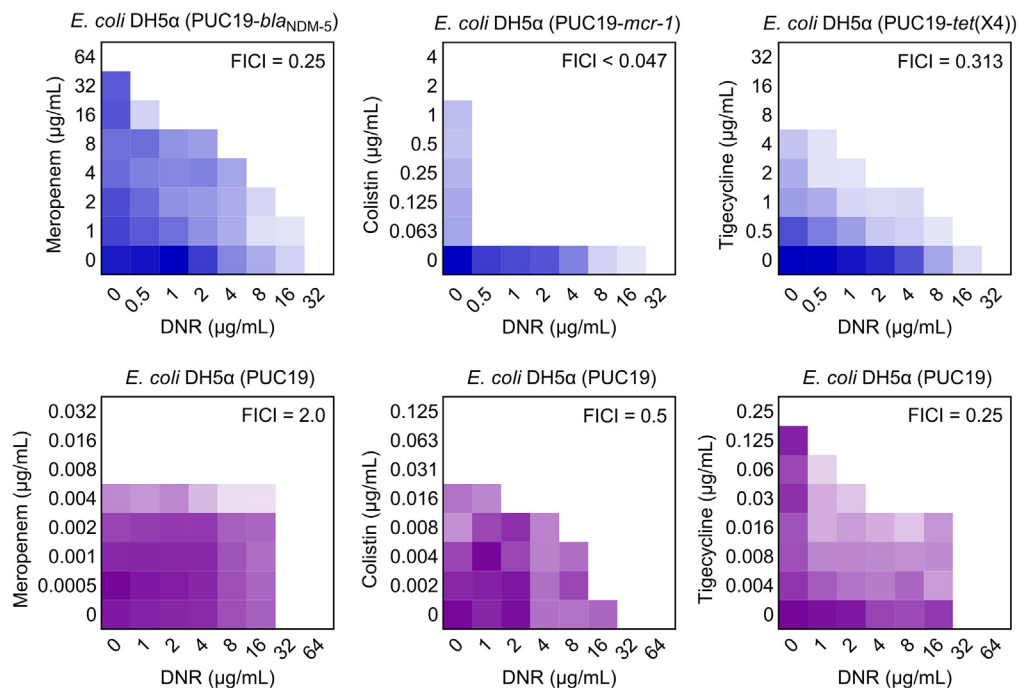


**Figure 2. Potentiating effect of DNR on three clinically important antibiotics against engineered drug-resistant and sensitive bacteria**

Dark blue areas show greater cell density. The data show the average optical density (OD) of two biological replicates (600 nm). An FIC index of less than 0.5 is used to define synergy.

DNR with meropenem, colistin, or tigecycline was only effective on resistant bacteria, we measured the potentiating activity of DNR in engineered *E. coli* DH5 $\alpha$  (PUC19-*bla*<sub>NDM-5</sub>/*mcr-1*/*tet*(X4)), empty *E. coli* DH5 $\alpha$  (PUC19) and two reference strains. Interestingly, we found that DNR and the above three antibiotics displayed strong synergistic activity against drug-resistant bacteria, while weak or even no synergistic activity for sensitive bacteria, implying that the inhibition of specific resistance determinants is related to the action of DNR (Figures 2 and S1). Furthermore, we evaluated the synergistic effects of DNR and colistin/tigecycline against four clinical isolates of drug-resistant pathogens, including *E. coli* G92 (*mcr-1*), *K. pneumoniae* D120 (*mcr-8*), *K. pneumoniae* YZSH26 (*tet*(X4)), and *Acinetobacter baumannii* C222 (*tet*(X6)). As expected, DNR substantially potentiated colistin/tigecycline activity against these clinical strains (Figure 3). Of particular note is colistin, whose minimum inhibitory concentrations (MICs) against mobile colistin resistance (MCR)-positive bacteria were drastically decreased from 4 to 0.004  $\mu$ g/mL (1,000-fold) at sub-inhibitory concentrations of DNR. Meanwhile, great potentiation of DNR to colistin/tigecycline was also observed in other tested *mcr-1* or *tet*(X4)-carrying clinical isolates (Figure S2). Consistently, the synergistic effect of DNR and colistin was higher than that of tigecycline, and the antibacterial activity of colistin was enhanced by more than 16-fold under one-quarter MIC of DNR.

The time-dependent killing curves of individual and combined drugs were performed to investigate their bactericidal effect. We found that the three drugs alone, including DNR, colistin, and tigecycline, displayed only slight bacteriostatic activity, while the combination of DNR with colistin/tigecycline greatly reduced the bacterial loads of *mcr/tet*(X)-positive strains in the exponential and stationary phase (Figure 4).

It is suggested that biofilms can greatly resist the bactericidal activity of antibiotics, thus leading to clinical failures.<sup>28,29</sup> In light of this, we next investigated the synergistic impact of DNR on the development of biofilm and the destruction of established biofilm using crystal violet staining. As shown in Figure 5A, we found that the presence of DNR greatly enhanced the inhibiting effect of antibiotics on biofilm formation compared to colistin/tigecycline alone. Notably, in the biofilm formation assays, low concentrations of drug combinations have no direct bactericidal activity, indicating that killing the bacteria was not the cause of the suppression of biofilm production at these doses. Moreover, the combined use of DNR and colistin/tigecycline also exhibited a synergistic effect in removing mature biofilms (Figure 5B). Among them, the

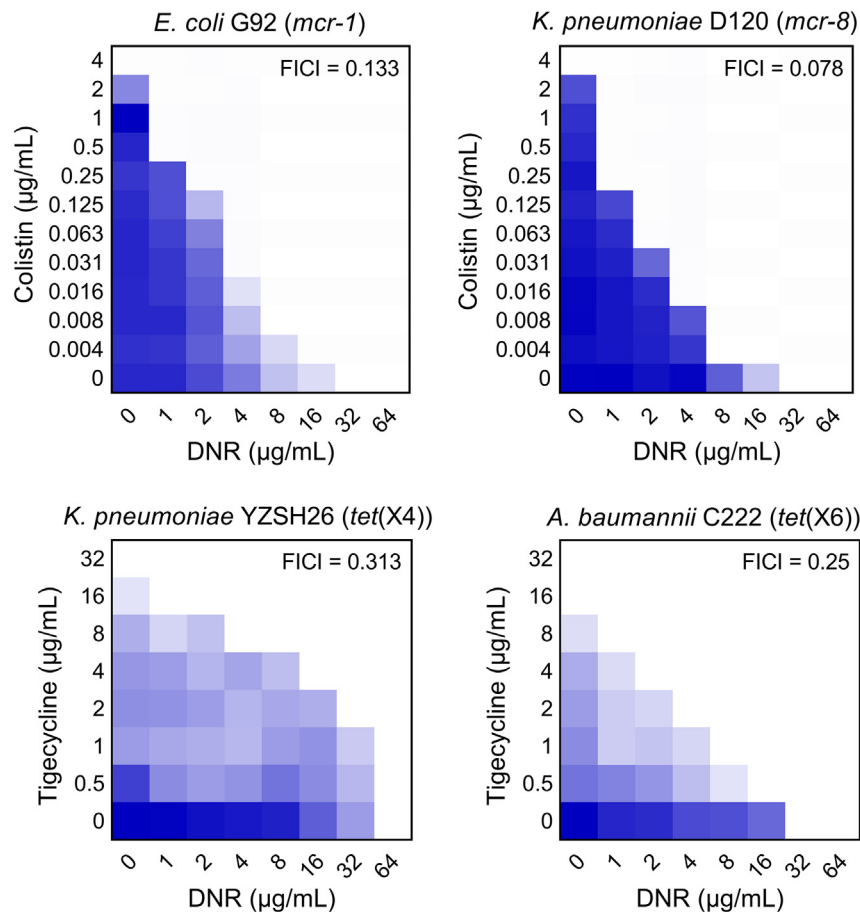


**Figure 3. Synergistic activity between DNR with colistin or tigecycline against clinical resistant strains**

Dark blue areas show greater cell density. The data show the average OD of two biological replicates (600 nm). An FIC index of less than 0.5 is used to define synergy.

combination of DNR and the highest concentration of colistin/tigecycline reduced the survival rate of biofilm bacteria to less than 1%. To sum up, these findings show that DNR effectively enhances the antibacterial activity of multiple last-resort antibiotics, particularly for colistin against MDR Gram-negative pathogens and biofilm-producing bacteria.

### Stability and safety evaluation of the combined use of DNR with colistin/tigecycline

Many candidate drugs are very active *in vitro* but work poorly *in vivo*, and the influence of various factors under physiological conditions may be an important reason.<sup>30</sup> To investigate the therapeutic potential of drug combinations,<sup>31</sup> we initially assessed the stabilization of DNR and colistin/tigecycline combinations in the existence of various salt ions and serum, which would affect the *in vivo* efficacy of medicines. After the addition of 10 mM Na<sup>+</sup>, K<sup>+</sup>, EDTA, 10% serum or 10% DMEM into the Mueller-Hinton Broth (MHB), the potentiation of DNR to antibiotics retained and more active in the presence of EDTA and serum; however, divalent ions such as 10 mM Ca<sup>2+</sup> and Mg<sup>2+</sup> caused the complete loss of the synergistic activity (FICI = 2.0) (Table S4). The alteration of activity in the existence of EDTA and divalent ions is closely related to bacterial membrane permeability,<sup>32</sup> suggesting that the synergistic effect of DNR with antibiotics may be associated with the damage of cell membrane.

Since the safety of drugs is of importance for translation application, we next assessed the hemolytic activity and acute toxicity of the drug combinations. As shown in Figure S3, the combined use of DNR (0–64 μg/mL) and colistin/tigecycline displayed a negligible hemolytic effect on mammalian RBCs, with a maximum of only about 2%. In addition, we examined the acute toxicity of DNR and colistin combination in a murine model. Compared with the colistin group, no significant body weight changes in mice after administration

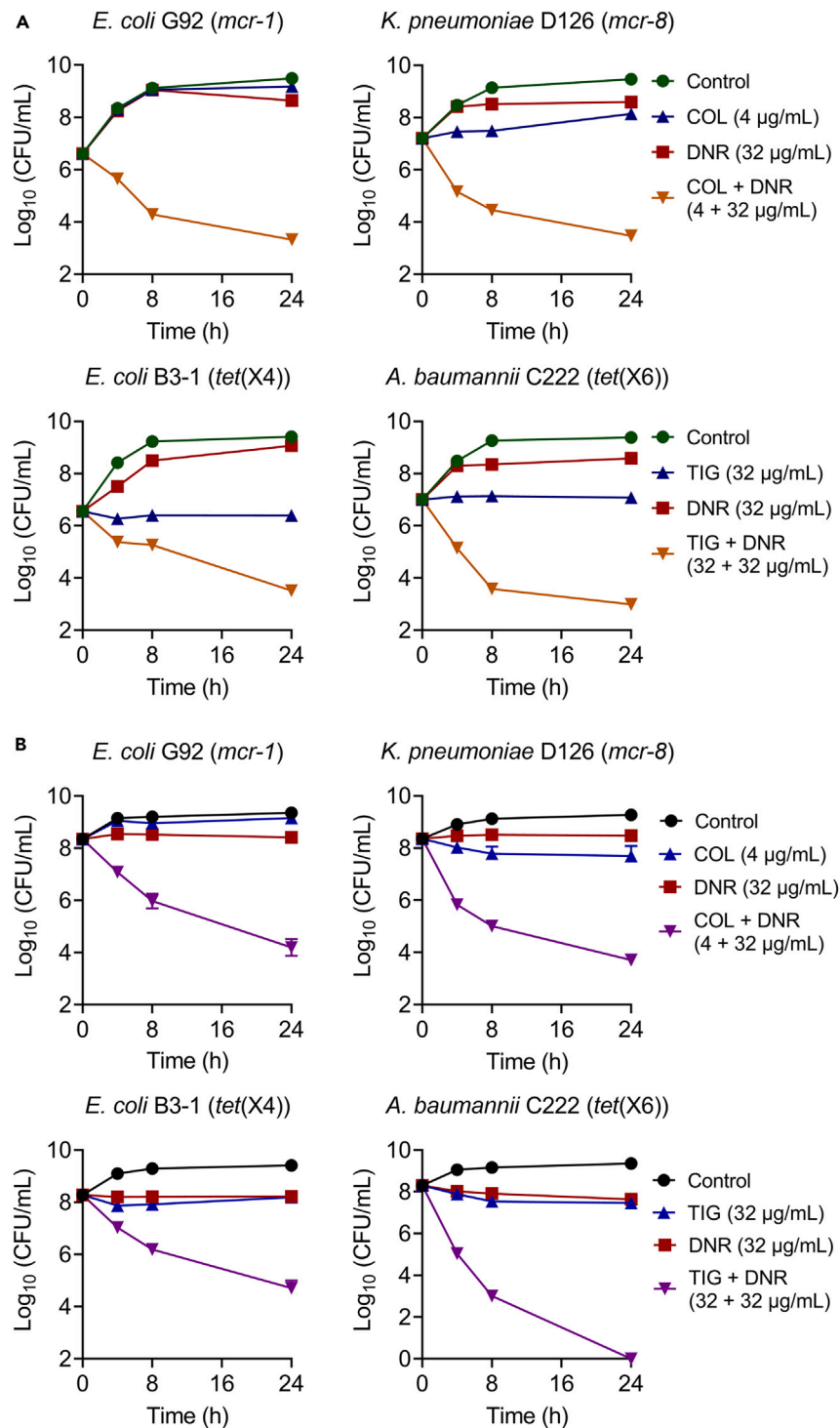


**Figure 4. DNR and colistin/tigecycline combinations display strong bactericidal activity against drug-resistant pathogens in exponential phase**

(A) and stationary phase (B) Time-kill curves of *E. coli* G92 (*mcr-1*), *K. pneumoniae* D120 (*mcr-8*), *E. coli* B3-1 (*tet(X4)*), and *A. baumannii* C222 (*tet(X6)*) in Luria-Bertani broth (LB) in the presence of DNR or colistin or tigecycline alone, or their combination during 24 h. Data were presented as mean  $\pm$  SD from three biological replicates. CFU, colony-forming unit.



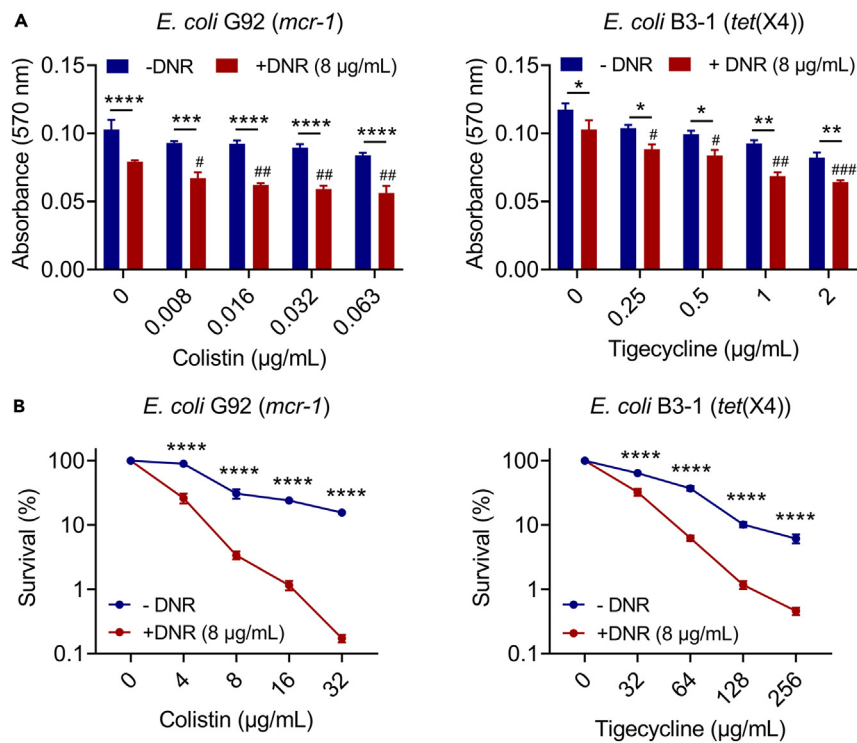


**Figure 5. Combined use of DNR and colistin/tigecycline effectively inhibits biofilm formation of drug-resistant bacteria and eliminates the mature biofilms**

Effects of DNR on the biofilm formation (A) and established biofilm eradication (B) of *E. coli* G92 (*mcr-1*) or *E. coli* B3-1 (*tet(X4)*) in the presence of increasing concentrations of colistin or tigecycline. Survival of biofilm-encased bacteria in (B) were normalized to blank control. Data were presented as mean  $\pm$  SD from three biological replicates, and statistical significance was determined by two-way ANOVA (\* $p < 0.05$ , \*\* $p < 0.01$ , \*\*\* $p < 0.001$ , \*\*\*\* $p < 0.0001$ ) or one-way ANOVA (colistin plus DNR versus DNR (8 µg/mL), # $p < 0.05$ , ## $p < 0.01$ , ### $p < 0.001$ ).

with DNR and colistin were observed (Figure S4). Additionally, blood routine and biochemical assays were also carried out. The blood-related parameters were all within the normal range (Tables S5 and S6). These results indicate that the combination of colistin/tigecycline and DNR displays superior antibacterial activity as well as biocompatibility even under physiological conditions.

### DNR suppresses the evolution and spread of mobile colistin/tigecycline resistance

In the long-term struggle with antibiotics, the bacterial resistance would continue to increase after a series of evolutions.<sup>33</sup> Therefore, using resistance development and mutation preventive concentration (MPC) assays, we investigated DNR's potential to prevent the evolution of colistin or tigecycline resistance. After 24 days of continuous passages, we found that DNR substantially slowed the increase of the MICs of colistin/tigecycline against passaged bacteria (Figure 6A). In addition, DNR supplementation dose-dependently reduced the MPC values of the two antibiotics against the corresponding resistant bacteria, implying that DNR can impede the emergence and evolution of colistin/tigecycline resistance (Figure 6B).

Considering that *mcr-1* and *tet(X4)* genes can spread widely by conjugative plasmids, ultimately conferring resistance to susceptible bacteria,<sup>34,35</sup> we next explored the effect of DNR on the conjugation frequency of colistin/tigecycline resistance plasmids. Interestingly, DNR significantly reduced the conjugation frequency of *mcr-1/tet(X4)*-harboring plasmids from clinical strains to the recipient bacteria *E. coli* EC600 in a concentration-dependent manner (Figures 7A and 7B). Furthermore, we evaluated the inhibitory effect of DNR on conjugal transfer in a murine model (Figure 7C). Consistently, the conjugation transfer frequency was also significantly reduced *in vivo* after DNR administration (Figures 7D and 7E). According to these findings, we conclude that DNR may be able to suppress the emergence and spread of mobile colistin/tigecycline resistance.

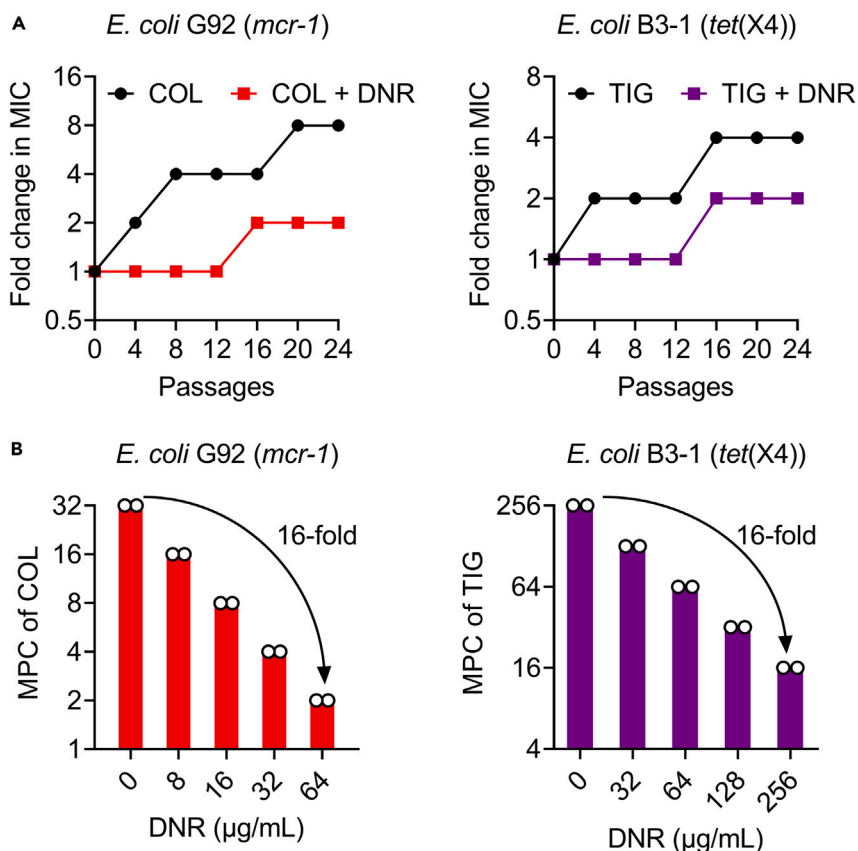


**Figure 6. DNR prevents the development of colistin/tigecycline resistance**

(A) Resistance development assays of *E. coli* G92 (*mcr-1*) and *E. coli* B3-1 (*tet(X4)*) after sequential passages with colistin or tigecycline alone or in combination with DNR, respectively.

(B) MPC values of colistin or tigecycline in the presence of increasing concentrations of DNR against *E. coli* G92 (*mcr-1*) and *E. coli* B3-1 (*tet(X4)*), respectively. Data were obtained from two biological replicates.

### Synergistic antibacterial mechanisms of DNR and colistin

Considering that colistin is a membrane-active antibiotic,<sup>36</sup> we first evaluated whether DNR could enhance the destructive activity of colistin on the cell membrane. Bacterial membrane integrity was determined using the propidium iodide (PI) probe, which can only cross the damaged membrane. Expectedly, DNR alone significantly increased the fluorescence value excited by PI dye in a concentration-dependent manner, and when it was used in combination with colistin, the fluorescence units were significantly higher than those of colistin or DNR acting alone (Figures 8A and 8B), indicating the enhanced membrane permeability under DNR and colistin combination. Consistently, increased  $\beta$ -galactosidase activity exposed to DNR or their combination was observed, demonstrating that  $\beta$ -galactosidase was released extracellularly due to membrane disruption (Figures 8C and 8D). In connection with the opposite effects of divalent cations and EDTA on the potentiation of DNR to colistin, we reasoned that the increased membrane permeability and membrane damage by DNR in colistin-resistant bacteria is of great importance for their synergistic activity. Given that DNR and colistin combination exhibited superior membrane disruption in *mcr-1*-positive bacteria, we further investigated the interaction between DNR and MCR-1 protein using *in silico* docking analysis. Interestingly, docking analysis using MCR-1 as receptor and DNR as ligand showed that DNR had a high affinity with MCR-1, with  $-11.3$  kcal/mol binding energies. Specifically, DNR can bind to MCR-1 protein by Van der Waals (Gly67, Ser89, Met265, and Asn267), hydrogen bond with Thr68, and pi-cation with Tyr72 (Figure 8E). In addition, we constructed point mutant strains at key sites and compared the synergy of DNR and colistin in these strains. The results showed that the synergistic effects of DNR with colistin against *E. coli* BL21 (pET28a) harboring the MCR-1 mutants (Ser89Ala, Pro266Ala, and Asn267Ala) were significantly reduced (Figure S5), indicating the important roles of these binding sites this interaction.



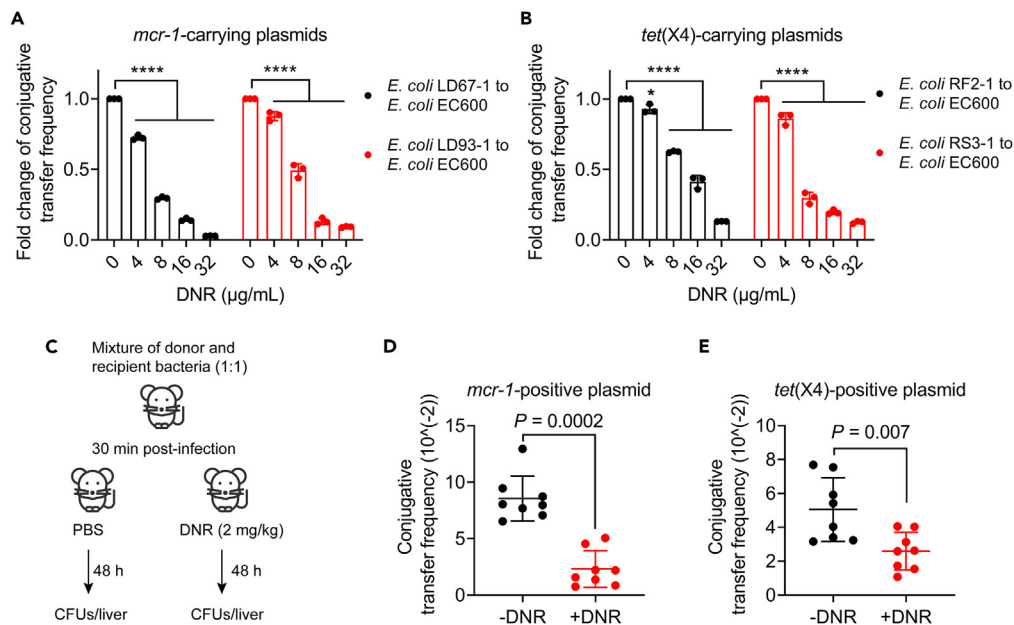


**Figure 7. DNR blocks the conjugative transfer of *mcr-1*/*tet(X4)*-carrying plasmids both *in vitro* and in murine models**

(A and B) Fold change (FC) of conjugative transfer frequency of *mcr-1*-carrying plasmids (A) or *tet(X4)*-carrying plasmids (B) from clinical isolates to the recipient bacteria *E. coli* EC600 in the presence of increasing concentrations of DNR. Data were shown as mean  $\pm$  SD, and statistical significance was determined by nonparametric one-way ANOVA.

(C) Schematic representation of conjugative transfer infection murine model.

(D and E) Conjugation frequency of *mcr-1*/*tet(X4)*-positive plasmids *in vivo* after treatment with DNR (2 mg/kg). Mann-Whitney U test was used to calculate *p* values.

In order to further explore the mechanisms of DNR and colistin synergism, we performed a transcriptomic analysis of *E. coli* G92 (*mcr-1*) after treatment with colistin alone or in combination with DNR. As a consequence, 243 up-regulated genes and 306 down-regulated genes were identified (Figure 9A). Gene ontology (GO) terms and kyoto encyclopedia of genes and genomes (KEGG) pathway enrichment analyses were applied to explore the roles of DEGs. SOS response, nitrate reductase complex, and nitrate reductase activity were the most common terms in biological process, cellular component, and molecular function enrichment (Figure 9B). Additionally, those significantly up-regulated genes were mainly involved in phenylalanine metabolism, galactose metabolism, nucleotide excision repair, and purine metabolism (Figure 9C), while the significantly down-regulated genes were enriched in nitrogen metabolism, quorum sensing, and ATP-binding cassette (ABC) transporter pathways (Figure 9D). The following RT-qPCR analysis indicated that the expression profiles of these representative genes in the above pathways were consistent with the transcriptional results (Figure S6A). Furthermore, DNR was revealed to inhibit the expression level of colistin resistance gene *mcr-1* in a concentration-dependent manner (Figure S6B), which further explains why DNR and colistin combination has a stronger synergistic activity against drug-resistant bacteria than sensitive bacteria.

Notably, the addition of DNR remarkably enhanced the SOS response of damaged bacteria, and the significantly up-regulated genes, including *recN*, *recA*, *dinB*, *dinI*, *sulA*, etc. were all involved in this function, implying that DNR may induce DNA damage. Thus, we next investigated the effect of DNR on bacterial DNA. Using RT-qPCR, we found that the expression of *recA* gene, which encodes a key protein participating in the homologous DNA repair process, was significantly up-regulated with increasing DNR concentration (Figure 10A). To verify these results, checkerboard assays and killing curves were performed in  $\Delta$ *recA* strain. As a result, stronger synergistic activity between DNR and colistin was observed in  $\Delta$ *recA* strains compared with the parent isolate (Figures 10B–10D), indicating that bacterial DNA damage contributes to their synergistic effect.

It has been demonstrated that DNA damage increases ROS production,<sup>37</sup> which is critical for the activity of bactericidal antibiotics. Thus, using the 2',7'-dichlorodihydrofluorescein diacetate (DCFH-DA) probe,

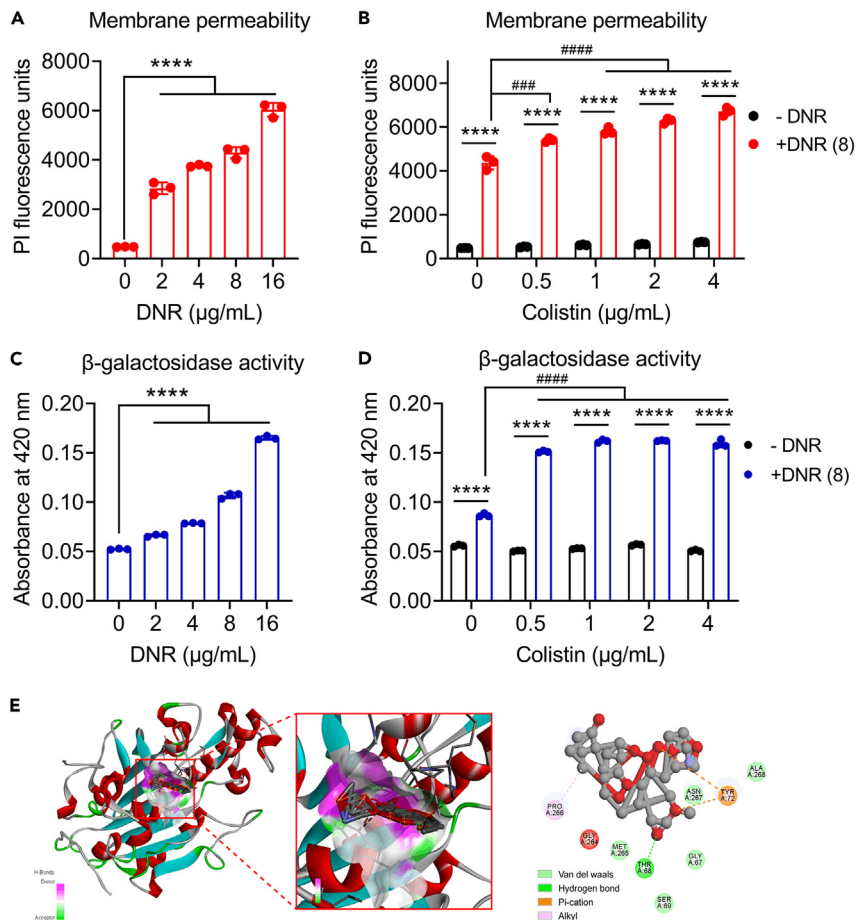


**Figure 8. DNR exacerbates bacterial membrane damage in together with colistin**

(A and B) Bacterial membrane permeability of *E. coli* G92 (*mcr-1*) exposed to DNR (A), colistin alone, or colistin plus DNR (8 µg/mL) (B).

(C and D) β-galactosidase activity in *E. coli* G92 (*mcr-1*) after exposure to DNR (C), colistin alone, or colistin plus DNR (8 µg/mL) (D). Data were presented as mean ± SD from three biological replicates. two-way ANOVA was used to evaluate statistical significance between colistin plus DNR and colistin (\*\*\*\**p* < 0.0001). Statistical significance of colistin plus DNR versus DNR (8 µg/mL) was determined by one-way ANOVA, and shown as ###*p* < 0.001, ####*p* < 0.0001.

(E) Interactions between DNR and the MCR-1 combining location residues.

we assessed the intracellular ROS levels in *E. coli* G92 treated with DNR or DNR plus colistin. As a result, we observed that DNR markedly and concentration-dependently boosted the generation of ROS. Higher ROS levels were also found under combined treatment than colistin or DNR alone (Figures 11A and 11B). To further demonstrate the roles of ROS generation in the synergism, *N*-acetyl-L-cysteine (NAC) and thiourea, two ROS scavengers, were introduced to the subsequent checkerboard experiments and time-dependent death assays, respectively. Consistently, the ROS scavengers significantly reduced the potentiation of DNR to colistin (Figures 11C and 11D). Collectively, these findings indicate that the combined use of DNR and colistin increases membrane damage and induces DNA damage and the massive production of ROS, thereby leading to bacterial cell death.

### DNR rescues colistin activity against drug-resistant bacteria *in vivo*

The effectiveness of this combination in one insect and two mammalian infection models was evaluated. Firstly, *E. coli* G92 (*mcr-1*) and *K. pneumoniae* D126 (*mcr-8*) were injected respectively to construct the infection models of *Galleria mellonella*, and then the larvae were treated individually or in combination. Although colistin alone was not effective in protecting *G. mellonella* larvae, combined treatments with colistin (1 or 5 mg/kg) and DNR (1 mg/kg) remarkably increased larval survival (Figures 12A and 12B). Additionally, a mouse model of peritonitis-sepsis elicited by *E. coli* G92 (*mcr-1*) further revealed the *in vivo*

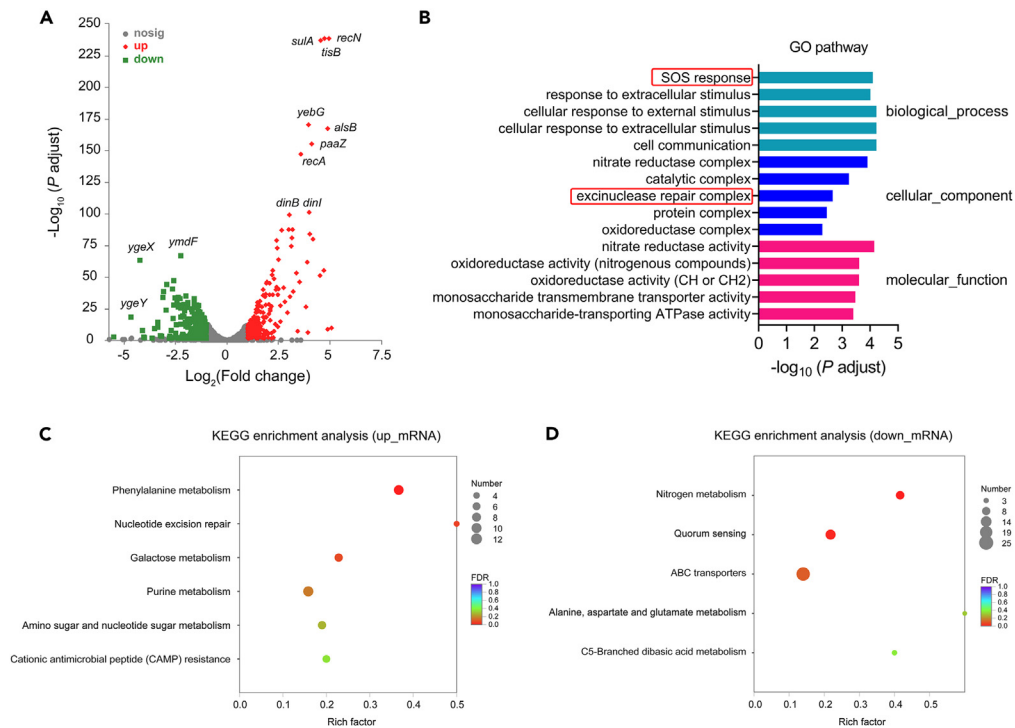


**Figure 9. Effect of DNR on mRNA expression in *mcr*-positive bacteria**

(A) Volcano maps of gene expression changes in *E. coli* G92 (*mcr-1*) after exposure to colistin plus DNR compared to colistin alone. Differentially expressed genes (DEGs) were identified by gene-expression-level analysis with  $p$  values of  $\leq 0.05$  and fold change values  $\geq 2$  ( $\log_2FC \geq 1$  or  $\log_2FC \leq -1$ ). (B) Gene ontology (GO) terms of significantly DEGs in *E. coli* G92 (*mcr-1*). (C and D) KEGG functional enrichment analysis of up-regulated (C) and down-regulated (D) genes.

synergy. A single dose of combined treatment increased the survival rate of mice, increasing to 50% and 75% under the action of colistin plus DNR (2 + 0.5 mg/kg, 2 + 1 mg/kg), respectively. By contrast, colistin or DNR monotherapy was not effective in treating severe infections caused by MCR-1-positive *E. coli* (Figure 12C). Finally, a neutropenic mouse infection model was used to evaluate this synergism. The loads of *mcr-1*-positive bacteria in the mouse thigh muscles were considerably reduced by two combined administrations of colistin plus DNR (2 + 0.5 mg/kg, 2 + 1 mg/kg) ( $p = 0.0022$  and  $p < 0.001$ , respectively) (Figure 12D). These data fully demonstrate that DNR restores the therapeutic effectiveness of colistin against *mcr*-positive bacterial infections *in vivo*.

## DISCUSSION

The increasing incidence of MDR-GN bacterial infections in the clinical setting has drastically compromised the efficacy of traditional antibiotic treatments. As a result, individuals with severe Gram-negative infections have limited therapy alternatives, which deepens the need for novel antibacterial strategies. Repurposing PACs as prospective antibiotic adjuvants is a promising pipeline to enhance the antibacterial activity of current antibiotics, decrease their dosages, and improve their biosafety by restoring the susceptibility of drug-resistant bacteria to antibiotics.<sup>38,39</sup> In this study, we demonstrated that the FDA-approved antineoplastic drug DNR is a potent and multifunctional adjuvant for three last-line antibiotics, including meropenem, colistin, and tigecycline, in fighting against *bla*<sub>NDM</sub>/*mcr*/*tet*(X)-harboring pathogens. Notably, the synergistic activity of DNR on colistin is superior to the other two antibiotics, with an increased activity up to 1,000-fold, indicating that DNR is a super colistin potentiator for MCR-positive bacteria. Furthermore, DNR significantly reduced the conjugative transfer of *mcr*/*tet*(X)-plasmids both *in vitro* and in a mouse model.

The mechanisms of action responsible for the potentiation of DNR to three antibiotics appear to be different. With regard to meropenem, we speculated that DNR may be a novel inhibitor of

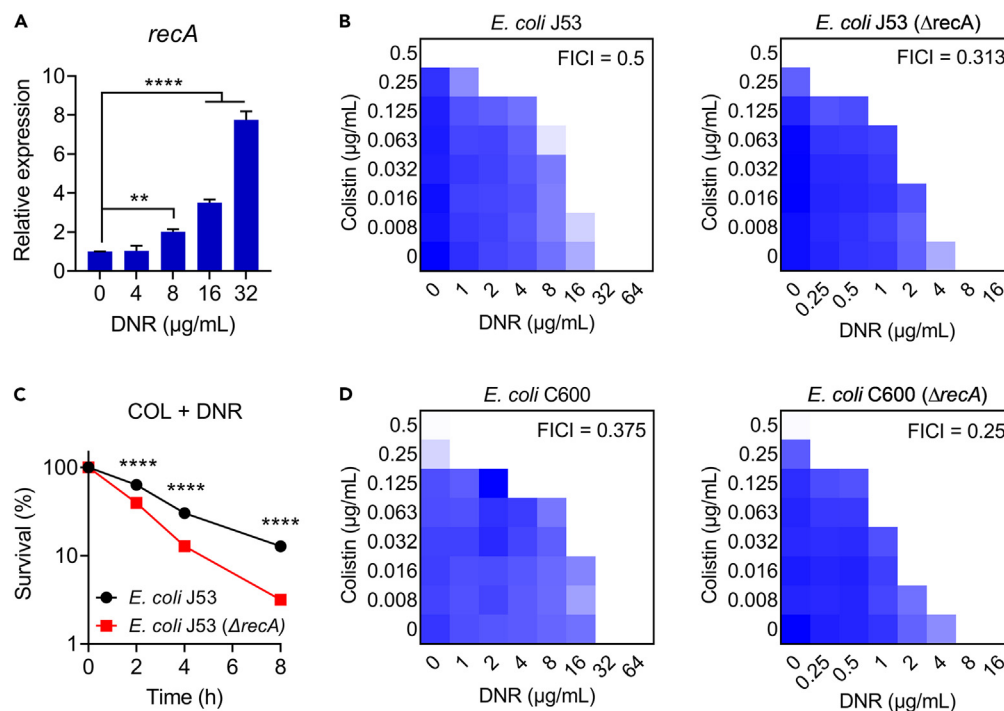


**Figure 10. DNR-induced DNA damage is critical for its synergistic activity with colistin**

(A) The expression levels of *recA* gene in *E. coli* G92 (*mcr-1*) after exposure to increasing concentrations of DNR. Data were shown as mean  $\pm$  SD, and nonparametric one-way ANOVA was used to assess the statistical significance (\*\* $p < 0.01$ , \*\*\*\* $p < 0.0001$ ).

(B) Synergistic activity between colistin and DNR against *E. coli* J53 and its *recA* knockout bacteria.

(C) The deletion of the *recA* gene in *E. coli* enhances the synergistic bactericidal activity between DNR and colistin.

(D) Checkerboard assay between DNR and colistin against *E. coli* EC600 and its *recA* knockout bacteria.

metallo- $\beta$ -lactamase because such synergism was only detected in NDM-positive bacteria. With regard to tigecycline, we suspect that it may be related to the different effects of DNR on protein because tigecycline exerts its bactericidal activity mainly by destroying protein. Considering the unprecedented potentiating effect of DNR on colistin, we sought to elucidate the underlying molecular mechanisms. Colistin is a membrane-disrupting antibiotic, and its antibacterial mechanism is currently known to be related to membrane damage.<sup>40</sup> In particular, colistin can specifically bind to lipopolysaccharides (LPS) located on the outer cell membrane, thereby resulting in membrane disruption. However, the *mcr-1* and its variations encoding phosphoethanolamine transferases decrease the negative charge of lipid A and enable bacteria resistant to colistin. Consistently, our study revealed that DNR significantly enhanced cell membrane permeability in MCR-positive bacteria. Heretofore, several compounds have been reported to restore the susceptibility of resistant bacteria to colistin, such as melatonin,<sup>41</sup> SLAP-25,<sup>42</sup> and PBT2,<sup>43</sup> by preventing the modification of lipid A by MCR-1. Our research also discovered that DNR can decrease the expression of resistance gene *mcr-1*, which in turn can reduce the modification of lipid A that MCR-1 causes. Moreover, docking analysis showed that DNR was a potential inhibitor of MCR protein. In line with these findings, DNR and colistin exhibited a more synergistic effect against *mcr*-positive bacteria than *mcr*-negative bacteria. In addition, we also found that DNR promoted DNA damage and massive production of ROS. Consistent with the antitumor mechanism of DNR-induced DNA double-strand breaks, DNR also caused significant DNA damage in prokaryotic cells. It has been demonstrated that DNA damage stimulates the creation of ROS and that within 2 h, the level of ROS in DNA-damaged cells grew dramatically, which can cause a death pathway resembling apoptosis.<sup>44</sup> Accordingly, DNA damage can cause the production of ROS through the H2AX-reduced coenzyme II oxidase 1 (Nox1)/Racl channel.<sup>45</sup> Of course, DNA damage and oxidative stress caused by ROS can promote each other, and excess ROS can in turn lead to DNA damage in various forms, such as double-strand breaks, double-strand aberrations, and site mutations. Nevertheless, the detailed mode of action between DNR and various antibiotics remains to be studied.

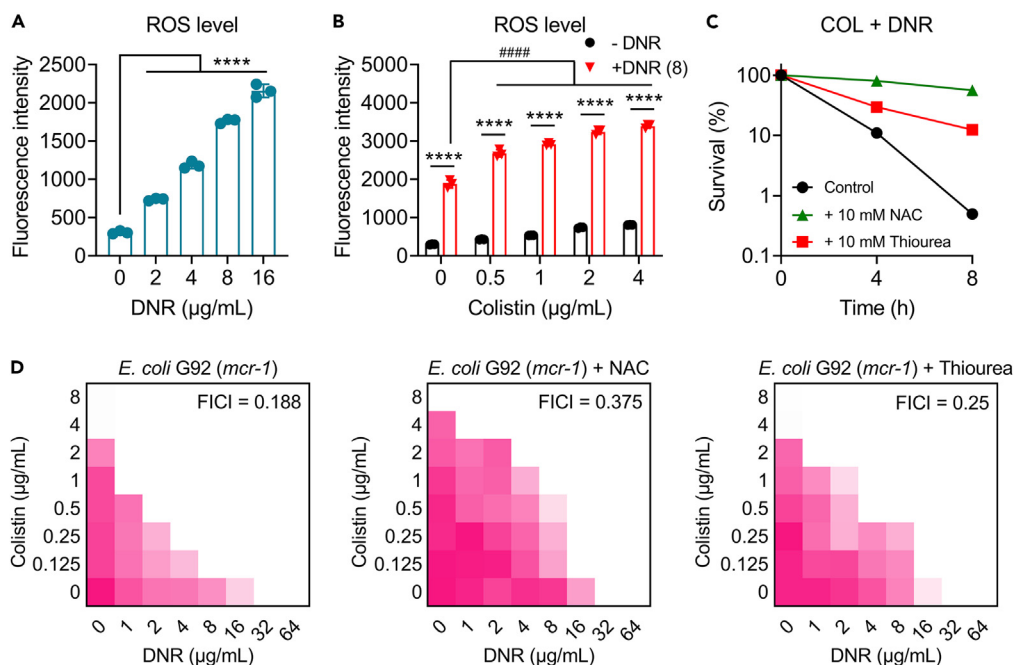


**Figure 11. DNR triggers oxidative damage in *mcr*-positive bacteria**

(A) Reactive oxygen species (ROS) generation in *E. coli* G92 (*mcr-1*) treated by varying concentrations of DNR.

Nonparametric one-way ANOVA was used to establish statistical significance (\*\*\*\* $p < 0.0001$ ).

(B) Combination of DNR (8  $\mu\text{g/mL}$ ) and colistin results in higher ROS generation than colistin or DNR alone. Statistical significance was determined by two-way ANOVA (\*\*\*\* $p < 0.0001$ ) or one-way ANOVA between colistin plus DNR and DNR (8  $\mu\text{g/mL}$ ) (### $p < 0.001$ ).

(C) The synergistic antibacterial effect of colistin and DNR is decreased in the presence of the ROS scavengers NAC or thiourea (10 mM).

(D) Checkerboard experiments of colistin and DNR against *E. coli* G92 (*mcr-1*) in the absence or presence of ROS scavengers NAC or thiourea (10 mM).

Acute toxicity tests showed that DNR (5 mg/kg) hardly increases the hepatic and renal toxicity of colistin. Moreover, our animal studies indicated that low doses of DNR (0.5 and 1 mg/kg) combined with colistin successfully treated drug-resistant bacterial infections, suggesting the therapeutic potential of this combination in clinical practice. To further improve drug efficacy and reduce the side effects of DNR, targeted drug delivery<sup>46</sup> and chemical structure optimization can be performed. For example, the toxicity of anti-tumor doxorubicin was significantly reduced when encapsulated in liposomes.<sup>47</sup> In addition, demethoxy DNR (idarubicin, IDA) with a removed methoxy group at the C<sub>4</sub> position remarkably improved its efficacy and reduced its toxicity.<sup>48</sup>

In conclusion, we reveal that DNR resensitizes MDR Gram-negative pathogens to the last-line antibiotics, and the synergism with colistin is the strongest. DNR significantly enhances membrane permeability of MCR-positive bacteria and induces DNA damage and oxidative stress. The synergistic effect of DNR and colistin is further evidenced in multiple animal models of infection. Together, our study provides a new drug combination strategy for the treatment of increasing MDR Gram-negative bacterial infections.

### Limitations of the study

In this study, although we have investigated the effectiveness of DNR and colistin in multiple animal models of infection, further work is still needed to verify the *in vivo* efficacy and safety of this combination therapy in clinical practice.

### STAR★METHODS

Detailed methods are provided in the online version of this paper and include the following:

- KEY RESOURCES TABLE

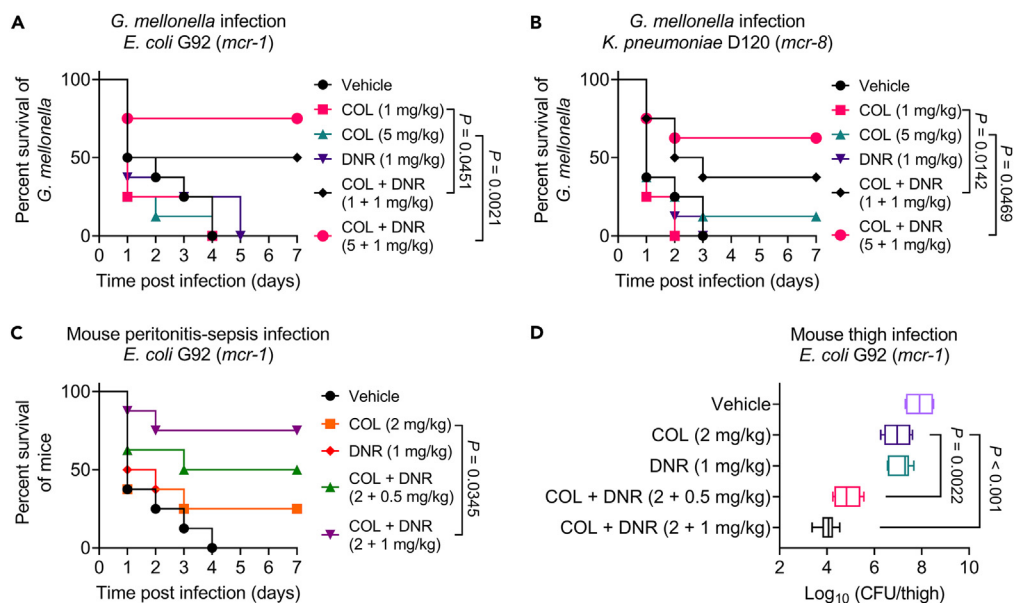


**Figure 12. Colistin and DNR combination is effective in one insect and two mammalian infection models**

(A and B) Survival rates of *G. mellonella* larvae ( $n = 8$  per group) infected by *E. coli* G92 (*mcr-1*) (A) or *K. pneumoniae* (*mcr-8*) (B) under the treatment of colistin (1 or 5 mg/kg), DNR (1 mg/kg) alone or in combination.  $p$  values were calculated using log rank (Mantel-Cox) test.

(C) Survival rates of infected mice ( $n = 8$  per group) treated by colistin (2 mg/kg), DNR (1 mg/kg), or their combination (2 + 0.5 or 2 + 1 mg/kg). The mice were infected by *E. coli* G92 (*mcr-1*).  $p$  values between COL and COL + DNR were calculated using log rank (Mantel-Cox) test.

(D) In comparison to colistin alone, the combination treatment of colistin and DNR considerably decreases bacterial burdens in the thighs of mice ( $n = 6$  per group). CFU, colony-forming unit.  $p$  values were determined by Mann-Whitney U test.

- **RESOURCE AVAILABILITY**

- Lead contact
- Materials availability
- Data and code availability

- **EXPERIMENTAL MODEL AND SUBJECT DETAILS**

- Bacterial strains and reagents
- Mice

- **METHOD DETAILS**

- Antibacterial test
- Checkerboard assay
- Time-dependent killing curves
- Toxicity analysis
- Biofilm inhibition assay
- Biofilm eradication assay
- Resistance development study
- Mutation preventive concentration assay
- Conjugation assays
- Membrane permeability and ROS level measurement
- $\beta$ -Galactosidase activity assay
- Docking analysis
- Transcriptomic analysis
- RT-qPCR analysis
- *Galleria mellonella* infection model
- Mouse peritonitis-sepsis infection model
- Neutropenic mouse thigh infection model

- **QUANTIFICATION AND STATISTICAL ANALYSIS**



## SUPPLEMENTAL INFORMATION

Supplemental information can be found online at <https://doi.org/10.1016/j.isci.2023.106809>.

## ACKNOWLEDGMENTS

This study was supported by the National Key Research and Development Program of China (2021YFD1801000 and 2018YFA0903400), National Natural Science Foundation of China (32222084, 32172907, and 32002331), Jiangsu Agricultural Science and Technology Innovation Fund (CX(21)2010), a project funded by the Priority Academic Program Development of Jiangsu Higher Education Institutions (PAPD) and 111 Project D18007.

## AUTHOR CONTRIBUTIONS

Y.L. and Z.W. designed and supervised the project. J.C. and T.D. performed experiment, analyzed data, and drafted the manuscript. J.S. helped perform experiments. C.C. helped analyze data. Y.L. and J.C. wrote and revised the manuscript. All of the authors read and approved the final manuscript.

## DECLARATION OF INTERESTS

The authors declare no competing interests.

## INCLUSION AND DIVERSITY

We support inclusive, diverse, and equitable conduct of research.

Received: August 31, 2022

Revised: February 26, 2023

Accepted: May 1, 2023

Published: May 4, 2023

## REFERENCES

- Kuehn, B. (2018). Antibiotic resistance challenge. *JAMA* 320, 1851.
- Antimicrobial Resistance Collaborators, Ikuta, K.S., Sharara, F., Swetschinski, L., Aguilar, G.R., Gray, A., Han, C., Bisignano, C., Rao, P., Wool, E., et al. (2022). Global burden of bacterial antimicrobial resistance in 2019: a systematic analysis. *Lancet* 399, 629–655.
- Domalaon, R., Idowu, T., Zhanel, G.G., and Schweizer, F. (2018). Antibiotic hybrids: the next generation of agents and adjuvants against Gram-negative pathogens? *Clin. Microbiol. Rev.* 31, 000777–000817.e117.
- MacNair, C.R., Tsai, C.N., and Brown, E.D. (2020). Creative targeting of the Gram-negative outer membrane in antibiotic discovery. *Ann. N. Y. Acad. Sci.* 1459, 69–85.
- Ropponen, H.K., Richter, R., Hirsch, A.K.H., and Lehr, C.M. (2021). Mastering the Gram-negative bacterial barrier - chemical approaches to increase bacterial bioavailability of antibiotics. *Adv. Drug Deliv. Rev.* 172, 339–360.
- Ruppé, É., Woerther, P.L., and Barbier, F. (2015). Mechanisms of antimicrobial resistance in Gram-negative bacilli. *Ann. Intensive Care* 5, 61.
- Kumarasamy, K.K., Toleman, M.A., Walsh, T.R., Bagaria, J., Butt, F., Balakrishnan, R., Chaudhary, U., Doumith, M., Giske, C.G., Irfan, S., et al. (2010). Emergence of a new antibiotic resistance mechanism in India, Pakistan, and the UK: a molecular, biological, and epidemiological study. *Lancet Infect. Dis.* 10, 597–602.
- Biswas, S., Brunel, J.M., Dubus, J.C., Reynaud-Gaubert, M., and Rolain, J.M. (2012). Colistin: an update on the antibiotic of the 21st century. *Expert Rev. Anti Infect. Ther.* 10, 917–934.
- Nang, S.C., Azad, M.A.K., Velkov, T., Zhou, Q.T., and Li, J. (2021). Rescuing the last-line polymyxins: achievements and challenges. *Pharmacol. Rev.* 73, 679–728.
- Stein, G.E., and Babinchak, T. (2013). Tigecycline: an update. *Diagn. Microbiol. Infect. Dis.* 75, 331–336.
- Liu, Y.Y., Wang, Y., Walsh, T.R., Yi, L.X., Zhang, R., Spencer, J., Doi, Y., Tian, G., Dong, B., Huang, X., et al. (2016). Emergence of plasmid-mediated colistin resistance mechanism MCR-1 in animals and human beings in China: a microbiological and molecular biological study. *Lancet Infect. Dis.* 16, 161–168.
- Sun, J., Chen, C., Cui, C.Y., Zhang, Y., Liu, X., Cui, Z.H., Ma, X.Y., Feng, Y., Fang, L.X., Lian, X.L., et al. (2019). Plasmid-encoded tet(X) genes that confer high-level tigecycline resistance in *Escherichia coli*. *Nat. Microbiol.* 4, 1457–1464.
- Czaplewski, L., Bax, R., Clokie, M., Dawson, M., Fairhead, H., Fischetti, V.A., Foster, S., Gilmore, B.F., Hancock, R.E.W., Harper, D., et al. (2016). Alternatives to antibiotics-a pipeline portfolio review. *Lancet Infect. Dis.* 16, 239–251.
- Baym, M., Stone, L.K., and Kishony, R. (2016). Multidrug evolutionary strategies to reverse antibiotic resistance. *Science* 351, aad3292.
- Payne, D.J., Gwynn, M.N., Holmes, D.J., and Pompliano, D.L. (2007). Drugs for bad bugs: confronting the challenges of antibacterial discovery. *Nat. Rev. Drug Discov.* 6, 29–40.
- Robbel, L., and Marahiel, M.A. (2010). Daptomycin, a bacterial lipopeptide synthesized by a nonribosomal machinery. *J. Biol. Chem.* 285, 27501–27508.
- Douafer, H., Andrieu, V., Phanstiel, O., 4th, and Brunel, J.M. (2019). Antibiotic adjuvants: make antibiotics great again. *J. Med. Chem.* 62, 8665–8681.
- Liu, Y., Li, R., Xiao, X., and Wang, Z. (2019). Antibiotic adjuvants: an alternative approach to overcome multi-drug resistant Gram-negative bacteria. *Crit. Rev. Microbiol.* 45, 301–314.
- Wright, G.D. (2016). Antibiotic adjuvants: rescuing antibiotics from resistance. *Trends Microbiol.* 24, 862–871.
- Ding, Y., Li, Z., Xu, C., Qin, W., Wu, Q., Wang, X., Cheng, X., Li, L., and Huang, W. (2021). Fluorogenic probes/inhibitors of beta-lactamase and their applications in

- drug-resistant bacteria. *Angew. Chem. Int. Ed.* 60, 24–40.
21. King, A.M., Reid-Yu, S.A., Wang, W., King, D.T., De Pascale, G., Strynadka, N.C., Walsh, T.R., Coombes, B.K., and Wright, G.D. (2014). Aspergillomarasmine A overcomes metallo-beta-lactamase antibiotic resistance. *Nature* 510, 503–506.
  22. Wang, R., Lai, T.P., Gao, P., Zhang, H., Ho, P.L., Woo, P.C.Y., Ma, G., Kao, R.Y.T., Li, H., and Sun, H. (2018). Bismuth antimicrobial drugs serve as broad-spectrum metallo-beta-lactamase inhibitors. *Nat. Commun.* 9, 439.
  23. Maiden, M.M., Hunt, A.M.A., Zachos, M.P., Gibson, J.A., Hurwitz, M.E., Mulks, M.H., and Waters, C.M. (2018). Triclosan is an aminoglycoside adjuvant for eradication of *Pseudomonas aeruginosa* biofilms. *Antimicrob. Agents Chemother.* 62, 001466-18–e218.
  24. Aubel-Sadron, G., and Londos-Gagliardi, D. (1984). Daunorubicin and doxorubicin, anthracycline antibiotics, a physicochemical and biological review. *Biochimie* 66, 333–352.
  25. Krauss, A.C., Gao, X., Li, L., Manning, M.L., Patel, P., Fu, W., Janoria, K.G., Gieser, G., Bateman, D.A., Przepiorka, D., et al. (2019). FDA approval summary: (daunorubicin and cytarabine) liposome for injection for the treatment of adults with high-risk acute myeloid leukemia. *Clin. Cancer Res.* 25, 2685–2690.
  26. Gumpert, J., Dornberger, K., and Smith, T.H. (1982). Antimicrobial activities of daunorubicin and adriamycin derivatives on bacterial and protoplast type L-form cells of *Bacillus subtilis* 170, *Escherichia coli* B, and *Proteus mirabilis* VI. Structure–activity relationship. *Z. Allg. Mikrobiol.* 22, 687–692.
  27. Hind, C.K., Dowson, C.G., Sutton, J.M., Jackson, T., Clifford, M., Garner, R.C., and Czaplewski, L. (2019). Evaluation of a library of FDA-approved drugs for their ability to potentiate antibiotics against multidrug-resistant Gram-negative pathogens. *Antimicrob. Agents Chemother.* 63, 007699–007719.e819.
  28. Koo, H., Allan, R.N., Howlin, R.P., Stoodley, P., and Hall-Stoodley, L. (2017). Targeting microbial biofilms: current and prospective therapeutic strategies. *Nat. Rev. Microbiol.* 15, 740–755.
  29. Yan, J., and Bassler, B.L. (2019). Surviving as a community: antibiotic tolerance and persistence in bacterial biofilms. *Cell Host Microbe* 26, 15–21.
  30. de Breij, A., Riool, M., Cordfunke, R.A., Malanovic, N., de Boer, L., Koning, R.I., Ravensbergen, E., Franken, M., van der Heijde, T., Boekema, B.K., et al. (2018). The antimicrobial peptide SAAP-148 combats drug-resistant bacteria and biofilms. *Sci. Transl. Med.* 10, eaan4044.
  31. Zipperer, A., Konnerth, M.C., Laux, C., Berscheid, A., Janek, D., Weidenmaier, C., Burian, M., Schilling, N.A., Slavetinsky, C., Marschal, M., et al. (2016). Human commensals producing a novel antibiotic impair pathogen colonization. *Nature* 535, 511–516.
  32. Liu, Y.F., Wang, L., Bu, C.P., Wang, G.Q., Zhang, Y.H., Fang, S.M., and Shi, W.Z. (2015). Synthesis of luminescent ag nanoclusters with antibacterial activity. *J. Nanomater.* 2015, 1–8.
  33. Wistrand-Yuen, E., Knopp, M., Hjort, K., Koskiniemi, S., Berg, O.G., and Andersson, D.I. (2018). Evolution of high-level resistance during low-level antibiotic exposure. *Nat. Commun.* 9, 1599.
  34. Li, R., Lu, X., Peng, K., Liu, Z., Li, Y., Liu, Y., Xiao, X., and Wang, Z. (2020). Deciphering the structural diversity and classification of the mobile tetracycline resistance gene tet(X)-bearing plasmidome among bacteria. *mSystems* 5, 001344–001420.e220.
  35. Wang, R., van Dorp, L., Shaw, L.P., Bradley, P., Wang, Q., Wang, X., Jin, L., Zhang, Q., Liu, Y., Rieux, A., et al. (2018). The global distribution and spread of the mobilized colistin resistance gene *mcr-1*. *Nat. Commun.* 9, 1179.
  36. Aslan, A.T., and Akova, M. (2022). The role of colistin in the era of new beta-lactam/beta-lactamase inhibitor combinations. *Antibiotics* 11, 277.
  37. Evert, B.A., Salmon, T.B., Song, B., Jingjing, L., Siede, W., and Doetsch, P.W. (2004). Spontaneous DNA damage in *Saccharomyces cerevisiae* elicits phenotypic properties similar to cancer cells. *J. Biol. Chem.* 279, 22585–22594.
  38. Bernal, P., Molina-Santiago, C., Daddaoua, A., and Llamas, M.A. (2013). Antibiotic adjuvants: identification and clinical use. *Microb. Biotechnol.* 6, 445–449.
  39. Liu, Y., Tong, Z., Shi, J., Li, R., Upton, M., and Wang, Z. (2021). Drug repurposing for next-generation combination therapies against multidrug-resistant bacteria. *Theranostics* 11, 4910–4928.
  40. Sabnis, A., Hagart, K.L., Klöckner, A., Becce, M., Evans, L.E., Furniss, R.C.D., Mavridou, D.A., Murphy, R., Stevens, M.M., Davies, J.C., et al. (2021). Colistin kills bacteria by targeting lipopolysaccharide in the cytoplasmic membrane. *Elife* 10, e65836.
  41. Liu, Y., Jia, Y., Yang, K., Tong, Z., Shi, J., Li, R., Xiao, X., Ren, W., Hardeland, R., Reiter, R.J., and Wang, Z. (2020). Melatonin overcomes MCR-mediated colistin resistance in Gram-negative pathogens. *Theranostics* 10, 10697–10711.
  42. Song, M., Liu, Y., Huang, X., Ding, S., Wang, Y., Shen, J., and Zhu, K. (2020). A broad-spectrum antibiotic adjuvant reverses multidrug-resistant Gram-negative pathogens. *Nat. Microbiol.* 5, 1040–1050.
  43. De Oliveira, D.M.P., Bohlmann, L., Conroy, T., Jen, F.E.C., Everest-Dass, A., Hansford, K.A., Bolisetti, R., El-Deeb, I.M., Forde, B.M., Phan, M.D., et al. (2020). Repurposing a neurodegenerative disease drug to treat Gram-negative antibiotic-resistant bacterial sepsis. *Sci. Transl. Med.* 12, eabb3791.
  44. Lam, S.J., O'Brien-Simpson, N.M., Pantarat, N., Sulistio, A., Wong, E.H.H., Chen, Y.Y., Lenzo, J.C., Holden, J.A., Blencowe, A., Reynolds, E.C., and Qiao, G.G. (2016). Combating multidrug-resistant Gram-negative bacteria with structurally nanoengineered antimicrobial peptide polymers. *Nat. Microbiol.* 1, 16162.
  45. Kang, M.A., So, E.Y., Simons, A.L., Spitz, D.R., and Ouchi, T. (2012). DNA damage induces reactive oxygen species generation through the H2AX-Nox1/Rac1 pathway. *Cell Death Dis.* 3, e249.
  46. Allen, T.M., and Cullis, P.R. (2013). Liposomal drug delivery systems: from concept to clinical applications. *Adv. Drug Deliv. Rev.* 65, 36–48.
  47. Batist, G., Ramakrishnan, G., Rao, C.S., Chandrasekharan, A., Guthel, J., Guthrie, T., Shah, P., Khojasteh, A., Nair, M.K., Hoelzer, K., et al. (2001). Reduced cardiotoxicity and preserved antitumor efficacy of liposome-encapsulated doxorubicin and cyclophosphamide compared with conventional doxorubicin and cyclophosphamide in a randomized, multicenter trial of metastatic breast cancer. *J. Clin. Oncol.* 19, 1444–1454.
  48. Fields, S.M., and Koeller, J.M. (1991). Idarubicin: a second-generation anthracycline. *DICP* 25, 505–517.
  49. Humphries, R., Bobenchik, A.M., Hindler, J.A., and Schuetz, A.N. (2021). Overview of changes to the clinical and laboratory standards institute performance standards for antimicrobial susceptibility testing, M100, 31st edition. *J. Clin. Microbiol.* 59, e0021321.
  50. Liu, Y., Jia, Y., Yang, K., Li, R., Xiao, X., and Wang, Z. (2020). Anti-HIV agent azidothymidine decreases Tet(X)-mediated bacterial resistance to tetracycline in *Escherichia coli*. *Commun. Biol.* 3, 162.
  51. Tong, Z., Xu, T., Deng, T., Shi, J., Wang, Z., and Liu, Y. (2021). Benzylamine reverses TMexCD-TOPJ-mediated high-level tetracycline resistance in Gram-negative bacteria. *Pharmaceuticals* 14, 907.
  52. Chen, S., Liu, D., Zhang, Q., Guo, P., Ding, S., Shen, J., Zhu, K., and Lin, W. (2021). A marine antibiotic kills multidrug-resistant bacteria without detectable high-level resistance. *ACS Infect. Dis.* 7, 884–893.
  53. Shi, J., Chen, C., Wang, D., Tong, Z., Wang, Z., and Liu, Y. (2021). Amphipathic peptide antibiotics with potent activity against multidrug-resistant pathogens. *Pharmaceuticals* 13, 438.
  54. Liu, Y., Tong, Z., Shi, J., Jia, Y., Deng, T., and Wang, Z. (2021). Reversion of antibiotic resistance in multidrug-resistant pathogens using non-antibiotic pharmaceutical benzylamine. *Commun. Biol.* 4, 1328.
  55. Mwangi, J., Yin, Y., Wang, G., Yang, M., Li, Y., Zhang, Z., and Lai, R. (2019). The antimicrobial peptide ZY4 combats multidrug-resistant *Pseudomonas aeruginosa* and *Acinetobacter baumannii* infection. *Proc. Natl. Acad. Sci. USA* 116, 26516–26522.

56. Deng, T., Jia, Y., Tong, Z., Shi, J., Wang, Z., and Liu, Y. (2022). Bismuth drugs reverse Tet(X)-conferred tigecycline resistance in Gram-negative bacteria. *Microbiol. Spectr.* *10*, e0157821.
57. Jia, Y., Yang, B., Shi, J., Fang, D., Wang, Z., and Liu, Y. (2022). Melatonin prevents conjugative transfer of plasmid-mediated antibiotic resistance genes by disrupting proton motive force. *Pharmacol. Res.* *175*, 105978.
58. Chen, X., Zhong, Z., Xu, Z., Chen, L., and Wang, Y. (2010). 2',7'-Dichlorodihydrofluorescein as a fluorescent probe for reactive oxygen species measurement: forty years of application and controversy. *Free Radic. Res.* *44*, 587–604.

## STAR★METHODS

## KEY RESOURCES TABLE

REAGENT or RESOURCE	SOURCE	IDENTIFIER
<b>Chemicals</b>		
Ampicillin	Yuanye Bio-Technology	Cat# S17018
Doxycycline	Yuanye Bio-Technology	Cat# S27317
Ciprofloxacin	Yuanye Bio-Technology	Cat# S17013
Vancomycin	Yuanye Bio-Technology	Cat# Y25829
Rifampicin	Yuanye Bio-Technology	Cat# B25308
Meropenem	Yuanye Bio-Technology	Cat# S31659
Colistin	Yuanye Bio-Technology	Cat# S17057
Tigecycline	Yuanye Bio-Technology	Cat# S24031
Daunorubicin	Yuanye Bio-Technology	Cat# S30893
PBS	Solarbio	Cat# P1020
LB Broth	Solarbio	Cat# L8291
MHB	Solarbio	Cat# M8556
LB agar	Solarbio	Cat# L8290
EDTA	Solarbio	Cat# E1007
Serum	Solarbio	Cat# S9040
DMEM	Solarbio	Cat# 12400024
Glycerol	Solarbio	Cat# G8192
Triton X-100	Solarbio	Cat# T8200
NaCl	Sigma	Cat# S9888
KCl	Sigma	Cat# P3911
MgCl <sub>2</sub>	Sigma	Cat# M8266
CaCl <sub>2</sub>	Sigma	Cat# C1016
N-acetylcysteine	Sigma	Cat# N7250
Thiourea	Sigma	Cat# T8656
Methanol	Sigma	Cat# 34860
Crystal violet	Sigma	Cat# C0775
Acetic acid	Sigma	Cat# 1005706
Propidium iodide	Sigma	Cat# P4170
DCFH-DA	Sigma	Cat# D6883
ONPG	Sigma	Cat# N1127
fresh sheep blood cells	Biofeng	Cat# A332-02
DMSO	Solarbio	Cat# D8372
<b>Critical commercial assays</b>		
EASYSpinPlus bacterial RNA extraction kit	Vazyme	Cat# 201-02
<b>Experimental models: Organisms</b>		
<i>G. mellonella</i> larvae	Huiyude Biotech Company	N/A
BALB/c or ICR mice	Comparative Medicine Center of Yangzhou University	N/A
<b>Software and algorithms</b>		
Autodock Vina	Autodock Vina software	<a href="https://vina.scripps.edu/">https://vina.scripps.edu/</a>
Prism version 9.0	GraphPad software	<a href="https://www.graphpad.com/">https://www.graphpad.com/</a>

(Continued on next page)

**Continued**

REAGENT or RESOURCE	SOURCE	IDENTIFIER
Other		
RNA-sequencing data	NCBI	PRJNA818073

**RESOURCE AVAILABILITY**

**Lead contact**

Further information and requests for resources and reagents should be directed to and will be fulfilled by the lead contact, Yuan Liu ([liuyuan2018@yzu.edu.cn](mailto:liuyuan2018@yzu.edu.cn)).

**Materials availability**

All unique/stable reagents used or generated in this study will be made available on request.

**Data and code availability**

- This paper does not report original code.
- RNA-sequencing data have been deposited in the National Center for Biotechnology Information (NCBI) Sequence Read Archive database (PRJNA818073) and are publicly available as of the date of publication.
- Any additional information required to reanalyze the data reported in this paper is available from the lead contact upon request.

**EXPERIMENTAL MODEL AND SUBJECT DETAILS**

**Bacterial strains and reagents**

Table S1 contains a list of the bacterial strains employed in this study. All tested strains were cultivated in a liquid medium, such as MHB, LB Broth, or LB agar plates. The strains that needed to be preserved were placed in 40% glycerol and stored at  $-80^{\circ}\text{C}$ .

**Mice**

Female BALB/c or ICR mice (6–8 weeks old) were purchased from Yangzhou University's Comparative Medicine Center (Jiangsu, China). The applicable regulations of the Jiangsu Laboratory Animal Welfare and Ethical of Jiangsu Administrative Committee of Laboratory Animals were followed in all mouse-related experiments (permission number, SYXKSU-2007-0005). Jiangsu Association for Science and Technology has granted SCXK-2017-0044 as the license number for the use of experimental animals.

**METHOD DETAILS**

**Antibacterial test**

Micro-broth dilution method, with reference to CLSI 2021,<sup>49</sup> was used to ascertain the MICs of drugs. In a 96-well plate containing cation-adjusted MH broth (MHB), a twofold dilution series of drug was prepared, and then an equal volume (100  $\mu\text{L}$ /well) of bacterial suspension ( $1.5 \times 10^6$  CFUs/mL) was added. The plates were then kept at  $37^{\circ}\text{C}$  for 18 h. The MICs were defined as the lowest concentration of compound at which no bacterial growth could be observed.

**Checkerboard assay**

Checkerboard experiment was used to investigate the synergistic activity between DNR and antibiotics according to our previous studies.<sup>50,51</sup> Briefly, antibiotics and DNR were diluted into 96-well plates in either horizontal or vertical coordinates, respectively. A microplate reader was used to measure the OD value at 600 nm following 18 h of culture at  $37^{\circ}\text{C}$  (The OD value greater than 0.1 indicates bacterial growth). FICI was calculated as the sum of  $\text{MIC}_{ab}/\text{MIC}_a$  and  $\text{MIC}_{ba}/\text{MIC}_b$ . MIC<sub>a</sub> and MIC<sub>b</sub> are the corresponding MICs of compounds A and B alone;  $\text{MIC}_{ab}$  is the MIC of compound A combined with compound B;  $\text{MIC}_{ba}$  is the MIC of compound B combined with compound A. Indicative of synergy is  $\text{FICI} \leq 0.5$ .

Checkerboard experiments were carried out to assess the impact of metal ions, EDTA, serum, and DMEM on the stability of the synergistic activity between DNR and colistin/tigecycline. In this process, the MHB containing 10 mM  $\text{Na}^+$ ,  $\text{K}^+$ ,  $\text{Ca}^{2+}$ ,  $\text{Mg}^{2+}$  or EDTA, 10% DMEM, 10% serum was used. To investigate the roles

of ROS production, ROS scavengers *N*-acetylcysteine (NAC, 10 mM) or thiourea (10 mM) were added to MHB. Furthermore, checkerboard assays of colistin and DNR against *E. coli* J53 and *E. coli* J53 ( $\Delta$ *recA*) were also performed.

### Time-dependent killing curves

Bactericidal curves of drugs against drug-resistant bacteria in the exponential and stationary phases were determined respectively.<sup>52</sup> Overnight *E. coli* G92 (*mcr-1*) and *E. coli* B3-1 (*tet(X4)*) was diluted 1:100 in MHB. Bacterial dilutions were cultured for 2 h (to exponential growth phase) and 4 h (to stationary phase), respectively. Subsequently, bacteria cells were treated with DNR (32  $\mu$ g/mL) or colistin (4  $\mu$ g/mL)/tigecycline (32  $\mu$ g/mL) alone or in combination, and a control group without drugs was set up. At each time point (0, 4, 8 and 24 h), 100  $\mu$ L of the bacterial culture was pipetted and continuously diluted 10-fold in PBS. The suspension was then plated onto LB agar plates and cultured for an overnight period at 37°C. The number of colonies was counted after 18 h of culture. The time-dependent killing curves of a reference strain *E. coli* J53 and *E. coli* J53 ( $\Delta$ *recA*) after exposure to the combination of DNR (32  $\mu$ g/mL) and colistin (4  $\mu$ g/mL) were also determined, respectively.

### Toxicity analysis

Hemolysis of drugs was measured based on our previous study.<sup>53</sup> Briefly, colistin (0 to 16  $\mu$ g/mL), tigecycline (0 to 128  $\mu$ g/mL), or the combination of colistin/tigecycline with DNR (0 to 64  $\mu$ g/mL) were applied to 8% of fresh sheep blood cells for 1 h at 37°C. Triton X-100 (0.2%) was chosen as a positive control and PBS was used as blank control. The formula below was used to calculate the hemolysis rate based on the absorbance of suspension at 576 nm:

$$\text{Hemolysis (\%)} = \left[ \frac{(\text{OD}_{576 \text{ sample}} - \text{OD}_{576 \text{ blank}})}{(\text{OD}_{576 \text{ Triton X-100}} - \text{OD}_{576 \text{ blank}})} \right] \times 100\%$$

Acute toxicity of colistin combined with DNR in mice was evaluated over 7 days.<sup>54</sup> BALB/c mice were randomly split into two groups ( $n = 8$  per group). A single dose of colistin (10 mg/kg) and a mixture of colistin and DNR (10 + 5 mg/kg) were intraperitoneally administered into mice. Survival of mice was monitored during 7 consecutive days, and the changes in body weight were recorded. On the 7th day, the mice blood was collected for following blood routine and biochemical parameters analysis.

### Biofilm inhibition assay

Crystal violet method was used to evaluate DNR's capacity to prevent the formation of biofilm.<sup>55</sup>

Colistin (0 to 0.063  $\mu$ g/mL), tigecycline (0 to 2  $\mu$ g/mL), or the combination of colistin/tigecycline and DNR (8  $\mu$ g/mL) were added to the *E. coli* G92 and *E. coli* B3-1 culture, respectively. After 48 h of incubation, cells were washed three times with 300  $\mu$ L PBS. Next, 200  $\mu$ L methanol was added to fix the cells for 15 min. After air-drying, 100  $\mu$ L 0.1% crystal violet was used to stain for 15 min. Stained biofilm was then rinsed with PBS three times and allowed to air dry naturally. Finally, 100  $\mu$ L of 33% glacial acetic acid was used to dissolve the stained biofilms. The absorbance of suspension at 570 nm was measured after 30 min of incubation at 37°C.

### Biofilm eradication assay

Overnight *E. coli* G92 and *E. coli* B3-1 were diluted 1:100 into LB broth and incubated for 4 h at 37°C. A 96-well flat-bottom plate was filled with an equal volume of MHB and 100  $\mu$ L of bacterial solution. The planktonic bacteria were removed after a 48-h incubation period at 37°C. Colistin (0 to 32  $\mu$ g/mL), tigecycline (0 to 256  $\mu$ g/mL), and 8  $\mu$ g/mL DNR were used to eliminate the mature biofilms, either alone or in combination. After 2 h incubation at 37°C, the remaining cells were dispersed by sonication for 20 min. The mixture was then redissolved, diluted and plated on LB agar plates overnight at 37°C. The colonies were counted after 18 h.

### Resistance development study

*E. coli* G92 and *E. coli* B3-1 overnight cultures were diluted 1:100 into LB broth containing 0.5  $\times$  MIC of colistin/tigecycline or combined with 0.25  $\times$  MIC DNR. After 12 h of incubation, bacterial culture was diluted 1:100 and added to a new medicated medium to continue the next generation. Every four passages, the MIC of the cultures was examined. The serial passaging was continued for 24 days.



### Mutation preventive concentration assay

Colistin/tigecycline or its combination with DNR were present at various concentrations on LB agar plates. On the corresponding resistant agar plates, 100  $\mu$ L of *E. coli* G92 and *E. coli* B3-1 ( $1.0 \times 10^{10}$  CFUs) were plated, and the plates were then incubated at 37°C. Bacterial growth was monitored after 72 h, and the drug's MPC was defined as the lowest concentration that could prevent resistance development (mutant colonies).<sup>56</sup>

### Conjugation assays

Conjugation assays were performed by measuring the conjugation frequency between donor and recipient in the absence or presence of DNR.<sup>57</sup> *E. coli* LD93-1 and *E. coli* LD67-1 were the *mcr-1* donors, whereas *E. coli* RS3-1 and *E. coli* RF2-1 were the *tet(X4)* donors. Bacteria were grown at 37°C until their OD<sub>600</sub> value reached 0.5. In a total amount of 2 mL, the donor and recipient were combined in a 1:1 ratio, and then various concentrations of DNR (0 to 32  $\mu$ g/mL) was added to the mixture. The mixture was serially diluted and plated on LB agar plates with single- or double-drug following an 18 h incubation period at 37°C. According to bacterial CFUs, conjugators and conjugation frequencies were calculated.

Referring to the above results, *E. coli* LD67-1 was chosen as the *mcr-1* donor, and *E. coli* RF2-1 was chosen as the *tet(X4)* donor for the following murine models. A 200  $\mu$ L injection of a mixture of donor and recipient microorganisms was given to female ICR mice (6-8 weeks old) in the right abdominal cavity. After 30 min infection, 200  $\mu$ L PBS or DNR (2 mg/kg) was intraperitoneally delivered (n = 8 per group), respectively. The mice were slaughtered by cervical dislocation 48 h after infection. To measure CFUs titers, the liver was removed, homogenized, continuously diluted, and plated on LB agar plates with single- or double-drugs.

### Membrane permeability and ROS level measurement

*E. coli* G92 overnight cultures were centrifuged and resuspended with PBS to obtain an OD<sub>600</sub> of 0.5. Then, fluorescent dyes were incubated with the bacterial suspension for 15 min at dark. 190  $\mu$ L of probe-labeled bacterial cells were placed to a 96-well plate after 30 min of incubation, then 10  $\mu$ L of colistin (0 to 4  $\mu$ g/mL), DNR (0 to 16  $\mu$ g/mL), or a combination of colistin and DNR (8  $\mu$ g/mL) were added. The fluorescence intensity was recorded after 1 h of incubation using a microplate reader (Tecan, Mannedorf, Switzerland).

#### Cell membrane integrity

To assess the integrity of the cell membrane, bacterial cells were stained with PI (0.5  $\mu$ M).<sup>42</sup> At wavelengths of 535 nm for excitation and 615 nm for emission, the fluorescence intensity was measured.

#### Total ROS production

2,7-Dichlorodihydrofluorescein diacetate (DCFH-DA, 10  $\mu$ M) was used to measure ROS levels.<sup>58</sup> Cells were rinsed three times with PBS and resuspended in PBS after being treated with ROS probes for 30 min. The fluorescence intensity was measured at the excitation wavelength of 488 nm and the emission wavelength of 525 nm.

### $\beta$ -Galactosidase activity assay

100  $\mu$ L suspension was taken after treatment with colistin (0 to 4  $\mu$ g/mL), DNR (0 to 16  $\mu$ g/mL), or a combination of colistin and DNR (8  $\mu$ g/mL) for 1 h. After adding 3 mM of O-nitrophenyl  $\beta$ -D-galactopyranoside (ONPG), the absorbance of suspension at 420 nm was measured following a 30-min incubation period at 37°C.

### Docking analysis

The crystal structure of the MCR-1 protein (PDB: 5YLF) was used as a template. Using the Autodock Vina tool, molecular docking between MCR-1 and DNR was carried out without the use of water molecules. Discovery Studio 4.5 displays the interactions of DNR with the residues of the binding sites in MCR-1 as a two-dimensional graphic. The MCR-1 mutants (Ser69Ala, Pro266Ala and ASN267Ala) were constructed in *E. coli* BL21 (pET28a-MCR-1) using optimized primers (Table S7).

### Transcriptomic analysis

Overnight *E. coli* G92 were diluted 1:100 in LB broth and cultured at 37°C for 2 h (until they reached the exponential phase). Then, cells were treated with colistin (4  $\mu$ g/mL) alone or in combination with DNR

(32 µg/mL) for 8 h. Total RNA was extracted using the EASYspinPlus bacterial RNA extraction kit. Subsequently, HiSeq2000 was sequenced with TruseqSBS kit v3HS (200 cycles) with a read length of  $2 \times 100$  (PE100). Filter the original sequencing readings and map the reference genome for *E. coli* K-12. Using the FPKM (Fragments Per Kilobase of transcript per Million mapped reads) method, differentially expressed genes with a *P*-value  $\leq 0.05$  and a FC value  $\geq 2$  ( $\log_2$  FC  $\geq 1$  or  $\log_2$  FC  $\leq -1$ ) were identified. Genes were then subjected to functional enrichment analysis, including GO enrichment and KEGG enrichment.

### RT-qPCR analysis

RT-qPCR analysis was performed by the SYBR Green I chimeric fluorescence method using the 7500 Fast Real-Time PCR System under the conditions of pre-denaturation (95°C, 30 s) and 40 cycles (95°C, 10 s; 60°C, 30 s). The change of mRNA expression after combined treatment was determined by  $2^{-\Delta\Delta C_t}$  method.

### *Galleria mellonella* infection model

*G. mellonella* larvae were randomly separated into four groups ( $n = 8$  per group), and subsequently infected with either *E. coli* G92 or *K. pneumoniae* suspension (10 µL,  $1.0 \times 10^5$  CFU per larva, respectively) at the right caudal foot. PBS, colistin (1 or 5 mg/kg), DNR (1 mg/kg), or colistin and DNR (1 + 1 mg/kg or 5 + 1 mg/kg) (10 µL) were administered to the larva's left caudal foot at one hour after infection, respectively. The survival rates of larvae were monitored regularly for 7 days.

### Mouse peritonitis-sepsis infection model

*E. coli* G92 suspension (200 µL,  $1.0 \times 10^8$  CFU per mouse) was intraperitoneally administered into female BALB/c mice ( $n = 8$  per group). At one-hour post-infection, PBS, colistin (1 mg/kg or 5 mg/kg), DNR (1 mg/kg), or the combination of colistin and DNR (1 + 1 mg/kg or 5 + 1 mg/kg) were intraperitoneally injected, respectively. The survival rates of mice were recorded continuously for 7 days.

### Neutropenic mouse thigh infection model

Female BALB/c mice ( $n = 6$  per group) were intraperitoneally injected with cyclophosphamide at doses of 150 and 100 mg/kg on days 4 and 1 before infection, respectively. *E. coli* G92 (100 µL,  $1.0 \times 10^5$  CFU per mouse) was then administered intramuscularly to the right thigh of mice. Then, 100 µL of PBS, colistin (2 mg/kg), DNR (1 mg/kg), or their combinations (2 + 0.5 mg/kg or 2 + 1 mg/kg) were administered intraperitoneally at one-hour post-infection. At 48 h post-infection, mice were slaughtered by cervical dislocation and the thigh muscles were removed, diluted and plated on LB agar plates. Following an 18 h incubation period at 37°C, bacterial colonies were counted accordingly.

## QUANTIFICATION AND STATISTICAL ANALYSIS

GraphPad Prism version 9.0 was used to analyze all data, which is displayed as mean  $\pm$  SD. Unpaired *t*-test or one-way ANOVA for multiple comparisons were carried out for the *in vitro* testing. In animal models, statistical significance of survival rate and bacterial load were analyzed by log-rank (Mantel-Cox) test or Mann-Whitney U test, respectively.  $P < 0.05$  was defined as a significant difference.